Ore Geology Reviews 161 (2023) 105633

Contents lists available at ScienceDirect

Ore Geology Reviews

journal homepage: www.elsevier.com/locate/oregeorev

Provenance of the Nb-rich bauxite and Li-rich claystone at the base of the Heshan Formation in Pingguo, Guangxi, SW China: Constrained by U–Pb ages and trace element contents of detrital zircon

Haonan Zhao [a,b], Kunyue Ling [b,*], Shengjiang Du [c], Hanjie Wen [d,e]

[a] School of Earth Sciences and Resources, China University of Geoscience, Beijing 100083, China
[b] State Key Laboratory of Ore Deposit Geochemistry, Institute of Geochemistry, Chinese Academy of Sciences, Guiyang 550081, China
[c] School of Mining Engineering, Guizhou Institute of Technology, Guiyang 550003, China
[d] School of Earth Science and Resources, Chang'an University, Xi'an 710054, China
[e] College of Earth and Planetary Sciences, University of Chinese Academy of Sciences, Beijing 100049, China

ARTICLE INFO

Keywords:
Detrital zircon
U-Pb dating
Niobium
Lithium
Heshan Formation

ABSTRACT

The base of the Upper Permian Heshan Formation in Pingguo County, Guangxi Province, SW China, can be divided into two layers: a lower Nb-rich bauxite layer and an upper Li-rich claystone layer. The sources of these layers may have played a critical role in their formation. Detrital zircon provenance analysis is an effective method for identifying sediment provenance; however, it has not been applied previously to the Nb-rich bauxite and Li-rich claystone, thus limiting our knowledge of the sources of these two layers. Detrital zircons from the bauxite and the claystone layers yield a single age peak at ~ 260 Ma, which is consistent with the age of the Emeishan Large Igneous Province (LIP; 263–257 Ma) and the Permian Palaeo-Tethyan magmatic arcs (300–260 Ma). In contrast, detrital zircons from the two layers yield different trace element signatures. Yttrium and Hf contents and U/Yb ratios of detrital zircon grains from the bauxite layer overlap with those of continental and oceanic crust and have similar Hf/Th, Th/Nb, Th/U, and Nb/Hf ratios to those of zircons of within-plate and magmatic arc origins. These results indicate that the bauxite was sourced from volcanic rocks or ash related to the Emeishan LIP and the Permian Palaeo-Tethyan magmatic arcs. However, detrital zircons from the claystone have similar Hf/Th, Th/Nb, Th/U, and Nb/Hf ratios to only those of zircon from magmatic arcs, suggesting a single Permian Palaeo-Tethyan magmatic arc source. Thus, our results reveal an abrupt change in the provenance of zircons at the base of the Heshan Formation. The lower Nb-rich bauxite layer was derived from the weathering of volcanic rocks or ash related to the Emeishan LIP and the Permian Palaeo-Tethyan magmatic arcs, whereas the upper Li-rich claystone layer was derived principally from the weathering of volcanic ash related to the Permian Palaeo-Tethyan magmatic arcs. Since Nb is an immobile element, volcanic rocks/ash related to the Emeishan LIP and the Permian magmatic arc could represent a source for bauxite and Nb. In contrast, Li is chemically highly mobile in the Earth's surface environment and its origin cannot be constrained easily, further work is needed to identify the sources of Li.

1. Introduction

Lithium is a critical metal and is used widely in the new energy industries, ceramics, and the chemical industry (Mao et al., 2019; Bowell et al., 2020). Niobium is also a critical metal and an indispensable raw material for the development of high-tech industries due to its high melting temperature and its use as a superconductor (Nico et al., 2016). Lithium and Nb resources are typically occurs in magmatic hydrothermal systems and are rare in sedimentary rocks (Wang et al., 2013). However, super-enrichment of Li and Nb has been identified in clastic sedimentary rocks at the base of the Heshan Formation in Pingguo County, Guangxi Province, SW China (Ling et al., 2021). These rocks are generally divided into two layers: a lower Nb-rich bauxite layer and an upper Li-rich claystone layer (Ling et al., 2021). Mineralogical, petrological, and geochemical studies have shown that Nb and Li are hosted mainly in anatase and cookeite, respectively (Ling et al., 2021;

* Corresponding author.
E-mail address: lingkunyue@mail.gyig.ac.cn (K. Ling).

https://doi.org/10.1016/j.oregeorev.2023.105633
Received 8 June 2023; Received in revised form 9 August 2023; Accepted 27 August 2023
Available online 28 August 2023

Zhao et al., 2022). Provenance analysis using immobile elements (Al, Ti, Nb, Ta, Zr, and Hf) has suggested that the bauxite was derived mainly from alkaline felsic rocks related to the Emeishan Large Igneous Province (LIP) whereas the claystone was derived mainly from peraluminous or moderately fractionated felsic rocks associated with Permian Palaeo-Tethyan magmatic arcs (Ling et al., 2021).

Detrital zircon provenance analysis has facilitated significant progress in the study of the provenance of the bauxite at the base of the Heshan Formation in western Guangxi Province (Deng et al., 2010; Yu et al., 2016; Hou et al., 2017; Yang et al., 2021). These studies have yielded consistent results with a single zircon age peak (256–261 Ma), which corresponding to the age of the Emeishan LIP (263–257 Ma) and/or Permian Palaeo-Tethyan magmatic arc-related volcanic rocks (300–260 Ma), including felsic rocks related to the Emeishan LIP (Deng et al., 2010), volcanic rocks related to Permian Palaeo-Tethyan magmatic arcs (Hou et al., 2017), and volcanic rocks related to both the Emeishan LIP and the Permian Palaeo-Tethyan magmatic arcs (Yu et al., 2016; Yang et al., 2021). Therefore, the link between these two volcanic events and the base of the Heshan Formation remains controversial and requires further research.

Previous studies have focused mainly on the sources of the bauxites rather than those of the claystones in the upper layer of the Heshan Formation. As the Nb-rich bauxites and the overlying Li-rich claystones in the Pingguo may have distinct sources (Ling et al., 2021), studying the provenance of the lower bauxite and upper claystone layers should improve our understanding of the links between volcanic eruptions and the formation of the base of the Heshan Formation.

2. Geological setting

The Youjiang Basin is located in western Guangxi on the southwestern margin of the South China Plate (Fig. 1A), between the Emeishan LIP (263–251 Ma) to the northwest and the Song Ma suture zone to the south (Genyao et al., 1999; Xu et al., 2001; Cai and Zhang, 2009; Shellnutt, 2014). During the Early Palaeozoic, the Yangtze Plate and the Indochina Block separated from Gondwana, drifted northward, and were subsequently subducted, forming Permian (277–252 Ma) island arcs, including those in the Truong Son belt. At the end of the Triassic, the plates amalgamated to form a single block, connecting along the Song Ma suture zone (Metcalfe, 2006; Halpin et al., 2016; Ke et al., 2018; Xu et al., 2020).

During the middle Permian, the Youjiang Basin comprised shallow carbonate platform and basinal depositional settings. On the platforms, the middle Permian Maokou Formation consists mainly of thick bioclastic carbonates and calcarenites. However, cherts, cherty shale, and carbonate were deposited in the basins (Shen et al., 2007). At the end of the middle Permian, the Dongwu orogeny led to domal uplift in the upper Yangtze region, causing a significant marine regression in southern China (Sun et al., 2010). The uplift is estimated to have been at least 450 m in the inner zone, 350 m in the intermediate zone, and 10–50 m in the outer zone of the Emeishan LIP (He et al., 2010). At the same time, massive volcanic eruptions occurred in the Emeishan LIP, covering an area of > 250,000 km^2 (Fig. 1A; Shellnutt, 2014). The greenhouse effect and acid rain caused by the eruptions increased continental weathering, and the weathered material was deposited in the Youjiang Basin to form the Wuchiapingian clastic sedimentary rocks in the Xuanwei, Longtan, and Heshan/Wuchiaping formations (Fig. 1B; Yu et al., 2019).

In western Guangxi, the erosion of Emeishan LIP volcanic rocks and uppermost limestone of the Maokou Formation provided a consistent source of sediment for the deposition of the bauxite and claystone at the base of the Heshan Formation, resulting in the Heshan Formation directly overlying the limestone of the Maokou Formation (Fig. 2; He et al., 2003, 2010; Fan et al., 2008; Liu et al., 2017; Yu et al., 2019). In the Pingguo area, the base of the Heshan Formation is subdivided into a lower layer (~8 m thick) of purple, grey, or black, Nb-rich bauxite ores (Fig. 3A–B, D, and E) and an overlying claystone (mudstone) layer (~10 m thick) consisting of black, carbonaceous, Li-rich claystones (Fig. 3A, C, D, F). The bauxite has Nb_2O_5 contents of 0.024–0.04 wt% (average = 0.034 wt%), while the claystone contains Li_2O concentrations of varying from 0.06 to 1.05 wt% (average = 0.45 wt%; Ling et al., 2021).

3. Sampling and methods

Representative bauxite (XX-Al) and claystone (JM-C) samples were collected from two sections at Xinxu village (XX) and Jiaomei village

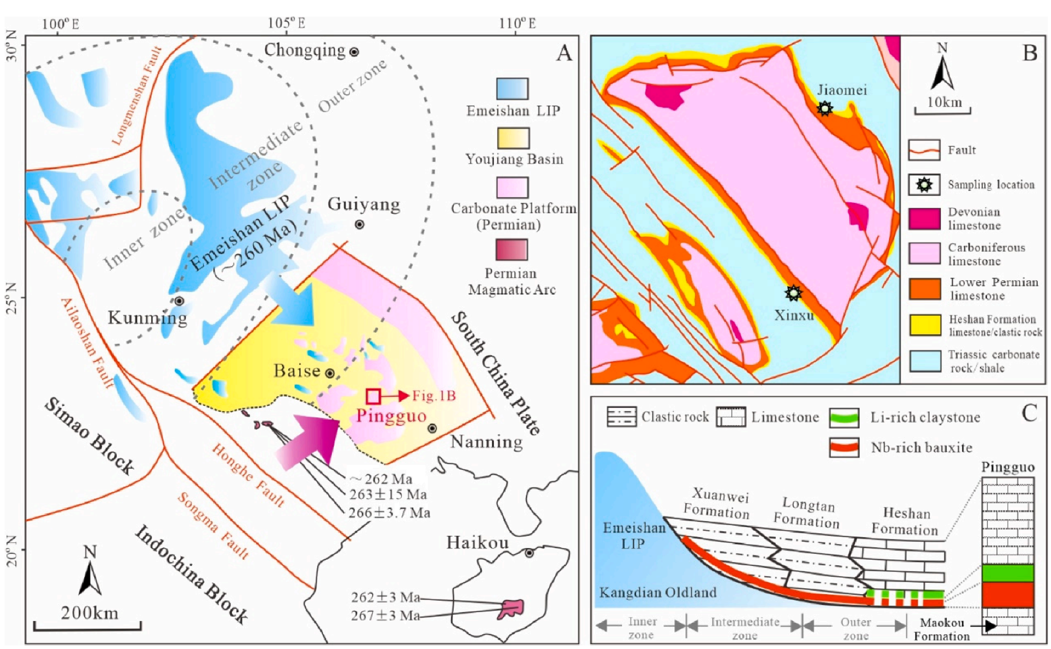

Fig. 1. (a) Simplified tectonic map of the South China Plate and showing the middle–late Permian palaeogeography of the Youjiang Basin (modified from He et al., 2003; Yu et al., 2019; Ling et al., 2021). (b) Geological map of the Pingguo area, Guangxi Province, SW China. (c) Palaeogeographic cross section for the period after formation of the Emeishan LIP, showing the location of the base of the Heshan Formation (modified from He et al., 2003).

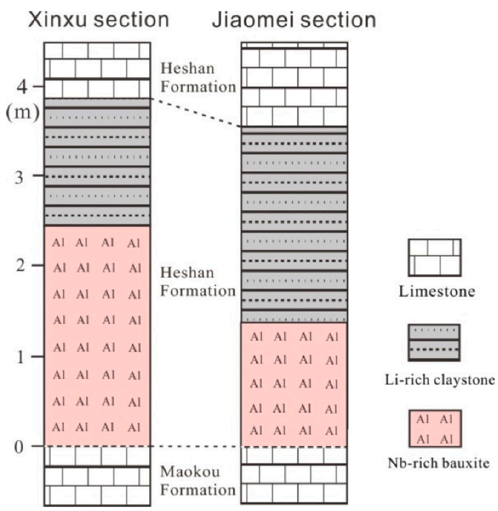

Fig. 2. Stratigraphic columns of the Xinxu and Jiaomei section in Pingguo County, Guangxi Province, SW China, illustrate the contact relationships between the depositional basement (paleo-karst), bauxite layer, and claystone layer.

(JM) in the Pingguo County (Fig. 1B and 3). Zircon grains were separated via conventional heavy liquid and magnetic techniques and were then hand-picked under a binocular microscope. Cathodoluminescence (CL) images of the zircon grains were used to select spots for U–Pb isotope analysis. The U–Pb ages and trace element compositions of zircon grains were determined by *in situ* laser ablation–inductively coupled plasma–mass spectrometry (LA-ICP-MS) analysis using an Agilent 7900 ICP–MS coupled with GeoasPro 193 nm laser at the Institute of Geochemistry, Chinese Academy of Sciences, Guiyang, China. The operating conditions and analytical procedures have been described in detail by Liu et al. (2008). Pre-defined areas of polished blocks were ablated using spots of 32 μm in diameter. The 91,500 zircon standard was used as an external standard to correct for isotopic fractionation in zircon. Zircon trace element analyses were calibrated using multiple reference materials (BCR-2G, BIR-1G, and BHVO-2G) without applying internal standardisation. Results of the U–Pb dating and trace element analyses are summarised in Tables S1–S2.

4. Results

4.1. Zircon morphology and trace element contents

Zircon grains from the two samples show similar morphologic features. Most are prismatic with lengths of 50–200 μm and aspect ratios of 1–5, suggesting relatively short transportation distances and little abrasion (Fig. 4). Oscillatory or cloudy zoning observed in CL images and high Th/U ratios (most > 0.1) indicate a magmatic origin.

LA–ICP–MS analyses of the zircon grains yielded high Hf (7297–24,663 ppm, with an average of 12,052 ppm), Th (16–1424 ppm, with an average of 260 ppm), U (18–2161 ppm, with an average of 492 ppm), and Y (365–3201 ppm, with an average of 2105 ppm) contents and low Nb (0.31–101 ppm, with an average of 4.88 ppm) and Ta (0.08–18.5 ppm, with an average of 1.63 ppm) contents. REE ranged from 645 to 10,602 ppm, with a mean of 1479 ppm. In addition, the heavy REE (HREE; 265–4306 ppm, with an average of 1447 ppm) contents of the grains are much higher than the light REE (LREE; 4–445 ppm, with an average of 32.9 ppm) contents.

4.2. U–Pb ages of the detrital zircons

A total of 200 valid ages were obtained from zircon grains from the two samples. 194 of them fall on or near the concordia trend (discordance $\leq 10\%$) and are displayed on relative probability plots and age histograms (Fig. 5). Age uncertainties for individual analyses are given as 1σ in the data table and concordia plots. The bauxite and claystone samples yield a single $^{206}Pb/^{238}U$ age peak at ~ 260 Ma (261–258 Ma). A few outliers that plot away from the concordia line yield scattered ages of 1867–310 Ma (Fig. 5A and C). In sample XX-Al, 98 out of 100 zircons have a mean age of 260.9 ± 1.6 Ma (MSWD = 1.20) (Fig. 5B). In sample JM-C, 96 out of 100 zircons have a mean age of 258.1 ± 2.9 Ma (MSWD = 1.30) (Fig. 5D).

5. Discussion

5.1. Provenance of the detrital zircon grains

5.1.1. Genesis of zircons

Zircon can be classified as being of magmatic, metamorphic, or hydrothermal origin based on its genesis (Lei et al., 2013). The zoning patterns and geochemical characteristics of zircon grains might indicate their origin (Crofu et al., 2003). Magmatic zircon grains generally have oscillatory zoning, high Th/U ratios (>0.1), and are enrichhed in HREEs

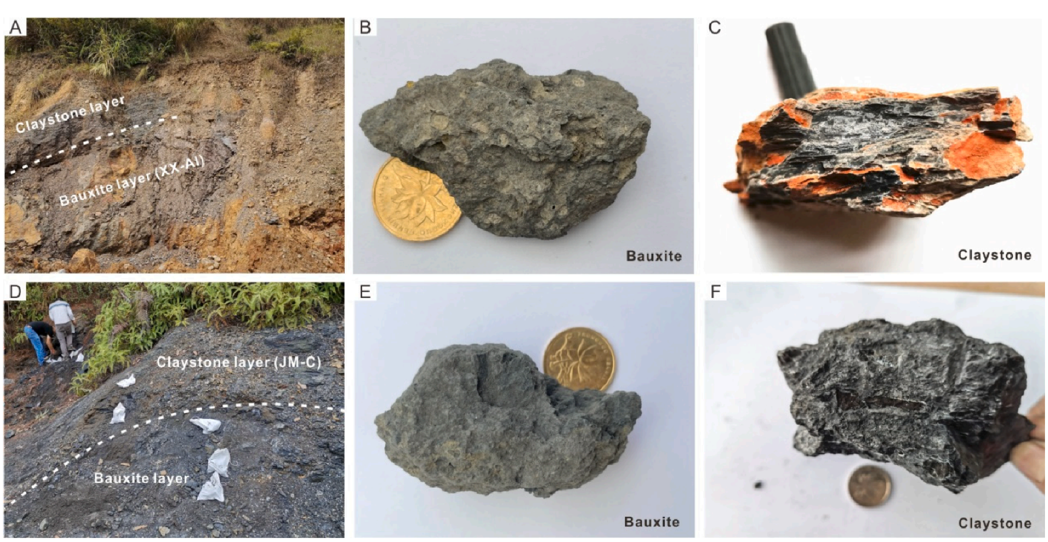

Fig. 3. Photos of the bauxite and claystone layers from the Pingguo area, western Guangxi Province, SW China. (A–C) Xinxu section; (D–F) Jiaomei section.

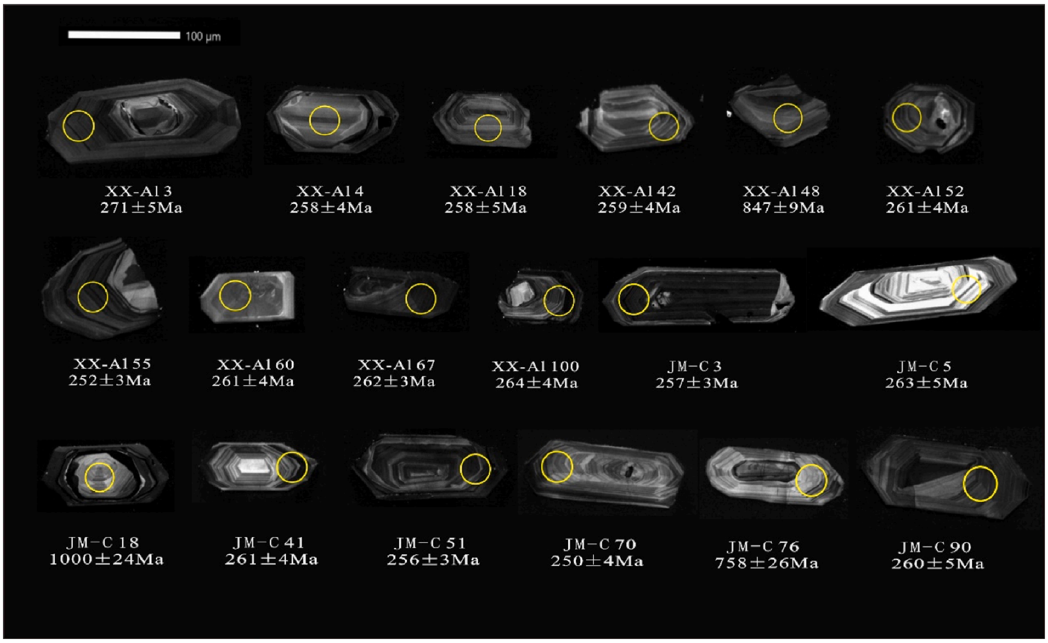

Fig. 4. Cathodoluminescence (CL) images of representative zircon grains. The yellow circles represent the locations of analysis spots for LA-ICP-MS. (For interpretation of the references to colour in this figure legend, the reader is referred to the web version of this article.)

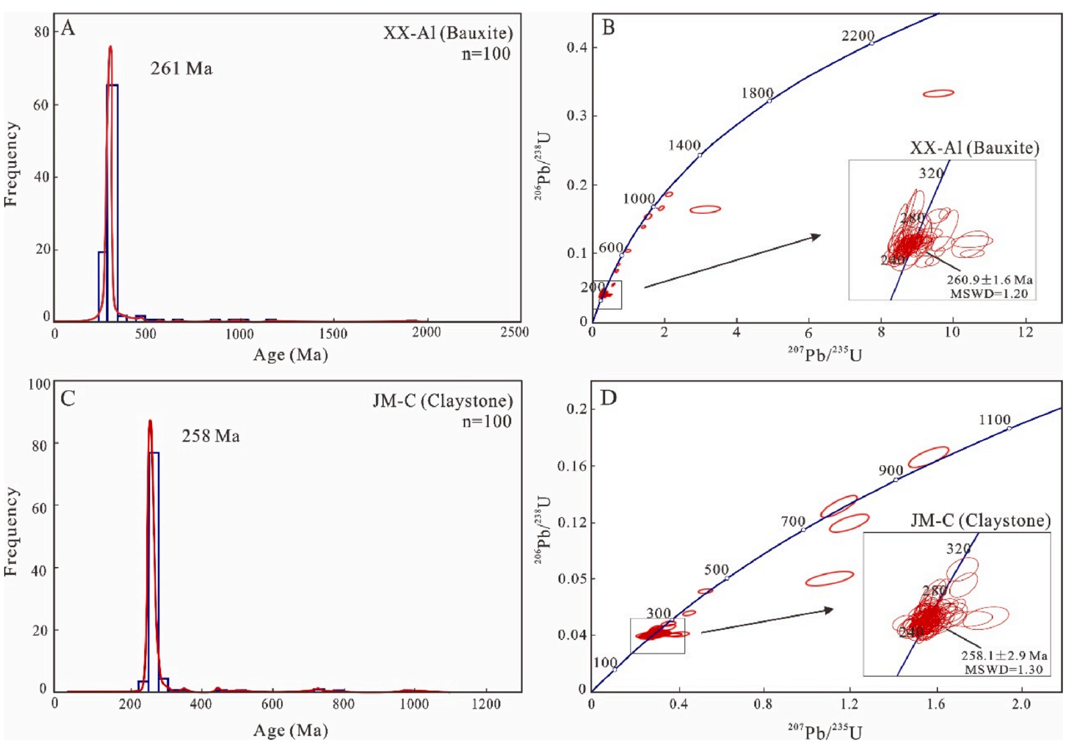

Fig. 5. Concordia diagrams and age histograms of detrital zircon U–Pb ages for samples XX-Al (A and B) and JM-C (C and D).

(Rubatto, 2002; Crofu et al., 2003; Hoskin and Schaltegger, 2003). In contrast, zircon grains with broad or unclear zoning and low Th/U ratios (<0.1) are usually found in metamorphic rocks (Hoskin, 2005). Hydrothermal zircon grains generally have flat LREE patterns and can be identified by morphological features, such as a homogeneous appearance in CL images or contained (hydrothermal) inclusions (Crofu et al., 2003).

The clear oscillatory zoning, high Th/U ratios (>0.1; Fig. 6), and high HREE contents suggest a magmatic origin for the detrital zircons in our samples. In addition, the abundance of prismatic shaped zircon grains suggests a proximal sediment source (Fig. 4).

5.1.2. *Source of zircons*

Detrital zircons from samples XX-Al and JM-C yield a single age peak at ~ 260 Ma (Fig. 5), which is consistent with the age of the Emeishan LIP (263–257 Ma; He et al., 2010; Yang et al., 2012) and falls within the reported range of the Permian Palaeo-Tethyan magmatic arcs (300–260 Ma; Halpin et al., 2016; Hou et al., 2017).

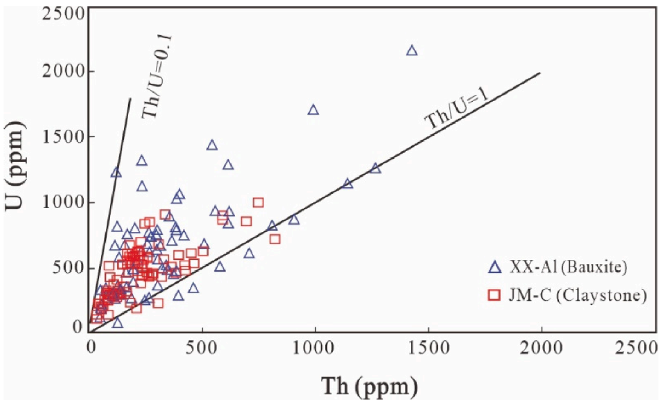

Fig. 6. The Th versus U diagram of the studied detrital zircons.

Zircon trace element contents are useful indicators of, for example, the nature of the magma source (Poitrasson et al., 2000). The detrital zircon grains from our samples plot both in the continental and the oceanic crust zircon fields on Y versus U/Yb, and Hf versus U/Yb diagrams (Fig. 7A–B), suggesting a mixed source. Th/U versus Nb/Hf, and Th/Nb versus Hf/Th diagrams can be used to determine, if zircons originate from within-plate/anorogenic and arc-related/orogenic settings (Zhong et al., 2013; Hou et al., 2014; Huang et al., 2014). In this study, rocks formed in a within-plate/anorogenic tectonic environment are from the Emeishan LIP, whereas those from arc-related/orogenic tectonic environments are associated with Permian magmatic arcs. Detrital zircons from the bauxite sample (XX-Al) plot in both the within-plate and the arc-related fields, indicating a mixed source (i.e., the Emeishan LIP and the Permian Palaeo-Tethyan magmatic arcs; Fig. 7). In contrast, detrital zircons from the Li-rich claystone sample (JM-C) plot only in the arc-related field, indicating a Permian magmatic arc provenance (Fig. 7C–D).

5.2. *Provenance of the bauxite and claystone*

Previous studies on detrital zircons in bauxites at the base of the Heshan Formation in western Guangxi area have suggested two main sediment sources: the Emeishan LIP-related volcanic rocks or ash and the Permian magmatic arc-related volcanic ash (Deng et al., 2010; Hou et al., 2014, 2017; Yu et al., 2016; Yang et al., 2021). In detail, detrital zircon studies of bauxites have revealed a dominant age peak at 261 ± 2 Ma and a negative Hf isotope composition ($\varepsilon_{Hf}(T)$ = -16.1 to −1.3), indicating that the primary sources of zircons are associated with the felsic rocks of the Emeishan LIP (Deng et al., 2010). However, Hou et al. (2017) argued that the $\varepsilon_{Hf}(T)$ values (-26.7 to −0.6) and trace element characteristics of detrital zircons in bauxites and clastic rocks were analogous to those of the Permian magmatic arc-related volcanic rocks (Hou et al., 2014, 2017). Recently, both the geochemical data obtained from bulk samples and detrital zircons of bauxites indicate a mixed provenance for the bauxite deposit, with metallogenic material derived from both felsic volcanic rocks of the Emeishan LIP and the Permian magmatic arc-related volcanic ash (Yu et al., 2016; Yang et al., 2021).

The main stage of volcanic activity of the Emeishan LIP occurred at ~ 260 Ma and its waning stage may have continued until ~ 257 Ma (Zhong et al., 2014). In this study, detrital zircons from the bauxite layer yield a dominant age peak at 260.9 ± 1.6 Ma (Fig. 5B), which corresponds to the volcanic peak of the Emeishan LIP, whereas those from the claystone layer yield a dominant age peak at 258.1 ± 2.9 Ma (Fig. 5D), which corresponds to the waning stage of the Emeishan LIP. This finding is consistent with the results obtained in a mercury study conducted by Ling et al. (2023), which observed abnormally high concentrations of Hg (indicating the peak of the Emeishan LIP) in the bauxite layer and moderately elevated levels of Hg (indicating the waning stage of the Emeishan LIP) in the claystone layer.

Given that massive volcanic eruptions (covering an area of > 250,000 km^2) occurred in the Emeishan LIP (Fig. 1A; Shellnutt, 2014), it is reasonable to hypothesise that volcanic rocks related to the Emeishan LIP could have provided sufficient material for the formation of the bauxite layer in the western Guangxi area (Deng et al., 2010). Further material may have been sourced from Permian magmatic arc-related volcanic rocks (Hou et al., 2014, 2017; Yu et al., 2016; Yang et al., 2021), as suggested by the ages and trace elements obtained for detrital zircons in this study. In contrast, detrital zircons from the claystone layer suggest a single source; i.e., Permian magmatic arc-related volcanic ash, as shown by the Th/U versus Nb/Hf, and Th/Nb versus Hf/Th diagrams

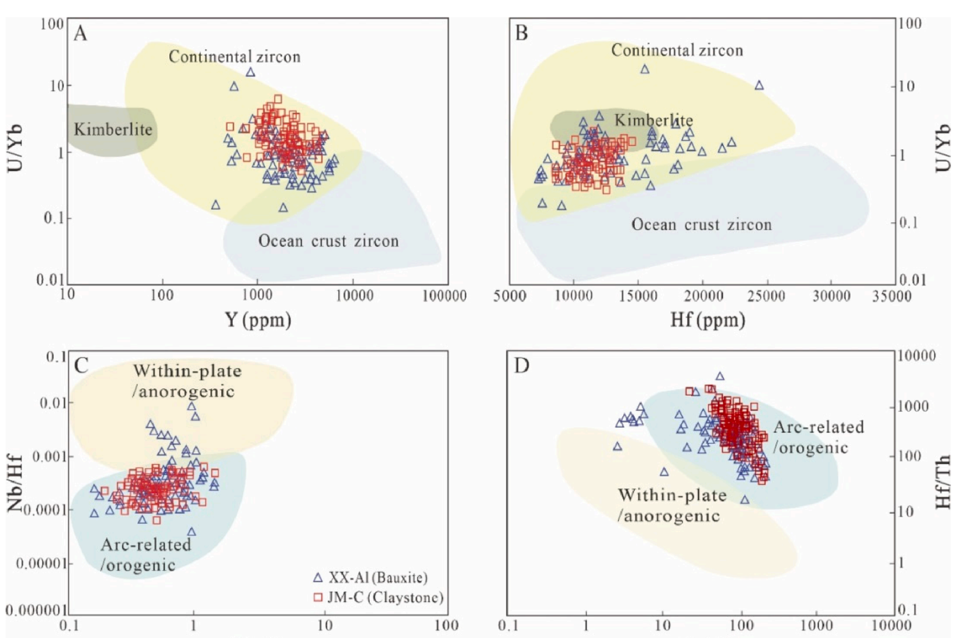

Fig. 7. (A) Y versus U/Yb, (B) Hf versus U/Yb (after Belousova et al., 2002; Grimes et al., 2007; Wang et al., 2015), (C) Th/U versus Nb/Hf, and (D) Th/Nb versus Hf/Th (Yang et al., 2012) diagrams of the studied zircon grains.

(Fig. 7C–D). Little to no sediment was supplied from the Emeishan LIP owing to weak volcanic activity during the waning stage of the Emeishan LIP. This abrupt change in provenance is consistent with the results obtained from the affinity anlaysis of immobile elements (Ling et al., 2021). The bauxite exhibits similar ratios of Al_2O_3/TiO_2, Nb/Ta, and Zr/Hf to those observed in alkaline felsic rocks associated with Emeishan LIP. In contrast, the claystone displays comparable ratios of Al_2O_3/TiO_2, Nb/Ta, and Zr/Hf to peraluminous or moderately fractionated felsic rocks related to the Permian Palaeo-Tethyan igneous arcs.

In summary, the geochemical compositions and ages of the detrital zircons suggest that the sources of the bauxite and the overlying claystone layers differ. The bauxite layer was derived mainly from volcanic rocks related to the Emeishan LIP and the Permian Palaeo-Tethyan magmatic arcs, whereas the claystone was derived largely from the Permian Palaeo-Tethyan magmatic arc rocks or ash. The abrupt change in the source during the deposition of the bauxite and claystone layers in the Pingguo area has been noted as well by Ling et al. (2021), who showed that there were large differences in the whole-rock immobile element contents (Zr, Hf, Nb, Ta) of the bauxites and claystone layers.

5.3. Implications to Nb and Li sources

Mineralogical and geochemical studies of the bauxite layer at the base of the Heshan Formation have suggested that Nb is mainly hosted in anatase (Ling et al., 2021; Zhao et al., 2022), which was either inherited from the parent rocks (the Emeishan LIP or the Permian magmatic arc) or formed through the transformation of Ti-rich minerals in the parent rocks. Therefore, volcanic rocks/ash may represent a source for bauxite and Nb in the Pingguo area. During weathering, sedimentary transport, and deposition of the source rocks, the immobile element Nb was preserved in Ti-rich minerals and gradually enriched in bauxite as weathering progressed.

In contrast, Li is an alkali element that is highly mobile in the Earth's surface environment. During chemical weathering, Li ions are discharged into water, which eventually flow into oceans/lakes or were bonded by clay minerals (Sun et al., 2018; Ling et al., 2021). We speculate that detritus of the Permian magmatic arcs could be a source for both the claystone layer and Li in the Pingguo area, because weathering of some felsic rocks/ash has the potential to give rise to Li-enriched rock formation. For example, in the McDermitt Li-clay deposit, Nevada, USA, a large amount of Li was leached from rhyolitic volcanic rocks and tephra by meteoric and hydrothermal fluids and then bounded into hectorite (a Li-bearing smectite) in tephra-rich sediments (Benson et al., 2017). However, further work is needed to identify the sources of Li.

5.4. Genesis of the Nb-rich bauxites and Li-rich claystones

Our results offer the following insights into the provenance of zircons of the two base layers of the Heshan Formation.

Stage 1: At the end of the middle Permian (~260 Ma), the Dongwu orogeny caused rapid uplift of the carbonate platform in the western Guangxi Province, which resulted in the exposure and intense weathering of limestone of the Maokou Formation, forming karst depressions and basins (Wang et al., 2020). Subsequent eruptions from the Emeishan LIP and the Permian Palaeo-Tethyan magmatic arcs released greenhouse gases (e.g., CO_2) and caused acid rain, resulting in enhanced continental weathering and the formation of Nb-rich bauxite in the karst depressions/basins (Fig. 8A–B).

Stage 2: The Emeishan LIP volcanism waned, whereas tephra related to Permian magmatic arcs was continuously deposited in the Pingguo area, followed by intense weathering, thus forming the Li-rich claystones above the bauxite layer (Fig. 8C).

6. Conclusions

Geochronologic and trace element analyses of detrital zircon grains from the base of the Heshan Formation in the Pingguo County, western Guangxi Province, SW China reveal an abrupt change in provenance between the lower Nb-rich bauxite and the overlying Li-rich claystone layers. The Nb-rich bauxite layer was derived from the weathering of volcanic rocks/ash related to the Emeishan LIP and the Permian Palaeo-Tethyan magmatic arcs, whereas the claystone layer was derived mainly from the weathering of volcanic ash related to the Permian Palaeo-Tethyan magmatic arcs.

Since Nb is an immobile element, volcanic rocks/ash related to the Emeishan LIP or the Permian magmatic arc could represent a source for bauxite and Nb in the Pingguo area. During the formation of the bauxite, Nb was preserved in Ti-rich minerals and gradually enriched in bauxite as weathering progressed. However, Li is highly chemically mobile in the Earth's surface environment and its origin cannot be easily constrained, further work is needed to identify the sources of Li.

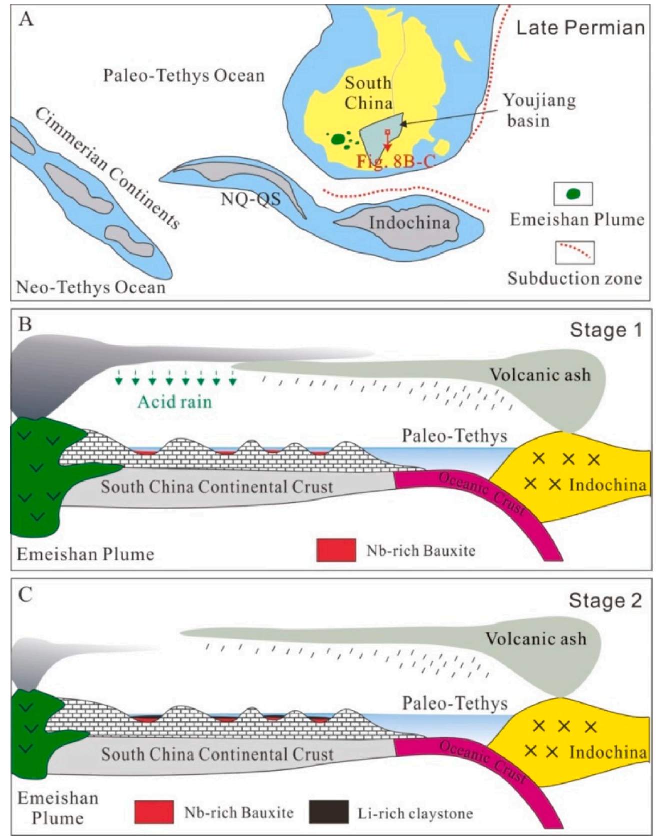

Fig. 8. Cartoon showing the formation of the two base layers of the Heshan Formation (modified from Wang et al., 2020; Yang et al., 2021). NQ-QS: North Qiangtang-Qamdo-Simao.

Declaration of Competing Interest

The authors declare that they have no known competing financial interests or personal relationships that could have appeared to influence the work reported in this paper.

Data availability

No data was used for the research described in the article.

Acknowledgements

This work was supported by the National Natural Science Foundation of China (grants 92062107, 92162214, 41903038, and 41962005), the Key R&D Program of the Yunan Province (grant 202103AQ100003), and the Guizhou Provincial Science and Technology Project (ZK[2021] key program 046).

Appendix A. Supplementary data

Supplementary data to this article can be found online at https://doi.org/10.1016/j.oregeorev.2023.105633.

References

Belousova, E., Griffin, W., O'Reilly, S.Y., Fisher, N., 2002. Igneous zircon: trace element composition as an indicator of source rock type. Contrib. Miner. Petrol. 143 (5), 602–622.

Benson, T.R., Coble, M.A., Rytuba, J.J., Mahood, G.A., 2017. Lithium enrichment in intracontinental rhyolite magmas leads to Li deposits in caldera basins. Nat. Commun. 8, 270.

Bowell, R.J., Lagos, L., de los Hoyos, C.R., Declercq, J., 2020. Classification and characteristics of natural lithium resources. Elements 16 (4), 259–264.

Cai, J.-X., Zhang, K.-J., 2009. A new model for the Indochina and South China collision during the Late Permian to the Middle Triassic. Tectonophysics 467 (1-4), 35–43.

Crofu, F., Hanchar, J.M., Hoskin, P.W.O., Kinny, P., 2003. Atlas of zircon textures. Rev. Mineral. Geochem. 53, 469–500.

Deng, J., Wang, Q., Yang, S., Liu, X., Zhang, Q., Yang, L., Yang, Y., 2010. Genetic relationship between the Emeishan plume and the bauxite deposits in Western Guangxi, China: constraints from U-Pb and Lu-Hf isotopes of the detrital zircons in bauxite ores. J. Asian Earth Sci. 37 (5-6), 412–424.

Fan, W., Zhang, C., Wang, Y., Guo, F., Peng, T., 2008. Geochronology and geochemistry of Permian basalts in western Guangxi Province, Southwest China: Evidence for plume-lithosphere interaction. Lithos 102 (1-2), 218–236.

Genyao, Wu, Dalai, Z., Qi, Z., Jianqing, Ji, 1999. Babu-Phu Ngu ophiolites: A geological record of Paleotethyan Ocean bordering China and Vietnam. Gondw. Res. 2 (4), 554–557.

Grimes, C.B., John, B.E., Kelemen, P.B., Mazdab, F.K., Wooden, J.L., Cheadle, M.J., Hanghøj, K., Schwartz, J.J., 2007. Trace element chemistry of zircons from oceanic crust: a method for distinguishing detrital zircon provenance. Geology 35, 643–646.

Halpin, J.A., Tran, H.T., Lai, C.K., Meffre, S., Crawford, A.J., Zaw, K., 2016. U-Pb zircon geochronology and geochemistry from NE Vietnam: A "tectonically disputed" territory between the Indochina and South China blocks. Gondw. Res. 34, 254–273.

He, B., Xu, Y.-G., Chung, S.-L., Xiao, L., Wang, Y., 2003. Sedimentary evidence for a rapid, kilometer-scale crustal doming prior to the eruption of the Emeishan flood basalts. Earth Planet. Sci. Lett. 213 (3-4), 391–405.

He, B., Xu, Y.-G., Zhong, Y.-T., Guan, J.-P., 2010. The Guadalupian-Lopingian boundary mudstones at Chaotian (SW China) are clastic rocks rather than acidic tuffs: Implication for a temporal coincidence between the end-Guadalupian mass extinction and the Emeishan volcanism. Lithos 119 (1-2), 10–19.

Hoskin, P.W.O., 2005. Trace-element composition of hydrothermal zircon and the alteration of Hadean zircon from the Jack Hills, Australia. Geochim. Cosmochim. Acta 69 (3), 637–648.

Hoskin, P.W.O., Schaltegger, U., 2003. The composition of zircon and igneous and metamorphic petrogenesis. Rev. Mineral. Geochem. 53 (1), 27–62.

Hou, Y.L., He, B., Zhong, Y.T., 2014. New perspective on provenance of the Permian karstic bauxite in the western Guangxi: geochemical evidence of clastic rocks of the Heshan Formation. Geotecton. Metallog. 38, 181–196 in Chinese with English abstract.

Hou, Y.L., Zhong, Y.T., Xu, Y.G., He, B., 2017. The provenance of late Permian karstic bauxite deposits in SW China, constrained by the geochemistry of interbedded clastic rocks, and U-Pb-Hf-O isotopes of detrital zircons. Lithos 278–281, 240–254.

Huang, H., Du, Y.S., Yang, J.H., Zhou, L., Hu, L.S., Huang, H.W., Huang, Z.Q., 2014. Origin of Permian basalts and clastic rocks in Napo, Southwest China: implications for the erosion and eruption of the Emeishan Large Igneous Province. Lithos 208–209, 324–338.

Ke, X., Zhang, Z., Yang, J., Yao, H., Zhu, L., He, W., 2018. Radiolarian and detrital zircon in the Upper Carboniferous to Permian Bancheng Formation, Qinfang Basin, and the geological significance. J. Earth Sci. 29 (3), 594–606.

Lei, W.Y., Shi, G.H., Liu, Y.X., 2013. Research progress on trace element characteristics of zircons of different origins. Geosci. Front. 20 (4), 273–284 in Chinese with English abstract.

Ling, K., Wen, H., Zhang, Q., Luo, C., Gu, H., Du, S., Yu, W., 2021. Super-enrichment of lithium and niobium in the upper Permian Heshan Formation in Pingguo, Guangxi, China. Sci. China Earth Sci. 64 (5), 753–772.

Ling, K., Wen, H., Grasby, S.E., Zhao, H., Deng, C., Yin, R., 2023. The Emeishan large igneous province eruption triggered coastal perturbations and the Capitanian mass extinction: Insights from mercury in Permian bauxite beds. Chem. Geol. 617, 121243.

Liu, Y., Hu, Z., Gao, S., Günther, D., Xu, J., Gao, C., Chen, H., 2008. In situ analysis of major and trace elements of anhydrous minerals by LA-ICP-MS without applying an internal standard. Chem. Geol. 257 (1-2), 34–43.

Liu, X., Wang, Q., Zhang, Q., Yang, S., Liang, Y., Zhang, Y., Li, Y., Guan, T., 2017. Genesis of the Permian karstic Pingguo bauxite deposit, western Guangxi, China. Miner. Deposita 52 (7), 1031–1048.

Mao, J.W., Yang, Z.X., Xie, G.Q., Yuan, S.D., Zhou, Z.H., 2019. Critical minerals: International trends and thinking. Miner. Deposits 38, 689–698 in Chinese with English abstract.

Metcalfe, I., 2006. Palaeozoic and Mesozoic tectonic evolution and palaeogeography of East Asian crustal fragments: The Korean Peninsula in context. Gondw. Res. 9 (1-2), 24–46.

Nico, C., Monteiro, T., Graça, M.P.F., 2016. Niobium oxides and niobates physical properties: Review and prospects. Progr. Mater. Sci. 80, 1–37.

Poitrasson, F., Chenery, S., Shepherd, T.J., 2000. Electron microprobe and LA-ICP-MS study of monazite hydrothermal alteration: Implications for U-Th-Pb geochronology and nuclear ceramics. Geochim. Cosmochim. Acta 64 (19), 3283–3297.

Rubatto, D., 2002. Zircon trace element geochemistry: partitioning with garnet and the link between U-Pb ages and metamorphism. Chem. Geol. 184 (1–2), 123–138.

Shellnutt, J.G., 2014. The Emeishan large igneous province: A synthesis. Geosci. Front. 5 (3), 369–394.

Shen, S.-Z., Wang, Y., Henderson, C.M., Cao, C.-Q., Wang, W., 2007. Biostratigraphy and lithofacies of the Permian System in the Laibin-Heshan area of Guangxi, South China. Palaeoworld 16 (1-3), 120–139.

Sun, Y., Lai, X., Wignall, P.B., Widdowson, M., Ali, J.R., Jiang, H., Wang, W., Yan, C., Bond, D.P.G., Védrine, S., 2010. Dating the onset and nature of the middle Permian Emeishan large igneous province eruptions in SW China using conodont biostratigraphy and its bearing on mantle plume uplift models. Lithos 119 (1-2), 20–33.

Sun, H.e., Xiao, Y., Gao, Y., Zhang, G., Casey, J.F., Shen, Y., 2018. Rapid enhancement of chemical weathering recorded by extremely light seawater lithium isotopes at the Permian-Triassic boundary. Proc. Nat. Acad. Sci. USA 115 (15), 3782–3787.

Wang, DengHong, Li, PeiGang, Qu, WenJun, Yin, LiJuan, Zhao, Z., Lei, ZhiYuan, Wen, ShenFu, 2013. Discovery and preliminary study of the high tungsten and lithium contents in the Dazhuyuan bauxite deposit, Guizhou, China. Sci. China Earth Sci. 56 (1), 145–152.

Wang, W., Liu, S., Santosh, M., Deng, Z., Guo, B., Zhao, Y., Zhang, S., Yang, P., Bai, X., Guo, R., 2015. Late Paleoproterozoic geodynamics of the North China craton: geochemical and zircon U-Pb-Hf records from a volcanic suite in the yanliao rift. Gondw. Res. 27 (1), 300–325.

Wang, Q., Yang, L., Xu, X., Santosh, M., Wang, Y., Wang, T., Chen, F., Wang, R., Gao, L., Liu, X., Yang, S., Zeng, Y., Chen, J., Zhang, Q., Deng, J., 2020. Multi-stage tectonics and metallogeny associated with Phanerozoic evolution of the South China Block: A holistic perspective from the Youjiang Basin. Earth Sci. Rev. 211, 103405.

Xu, Y., Chung, S.-L., Jahn, B.-M., Wu, G., 2001. Petrologic and geochemical constraints on the petrogenesis of Permian-Triassic Emeishan flood basalts in southwestern China. Lithos 58 (3-4), 145–168.

Xu, J., Xia, X.-P., Cai, K., Lai, C.-K., Liu, X.-J., Yang, Q., Zhou, M.-L., Ma, P.-F., Zhang, L. e., 2020. Remnants of a Middle Triassic island arc on western margin of South China Block: Evidence for bipolar subduction of the Paleotethyan Ailaoshan Ocean. Lithos 360-361, 105447.

Yang, J., Cawood, P.A., Du, Y., Huang, H., Huang, H., Tao, P., 2012. Large Igneous Province and magmatic arc sourced Permian-Triassic volcanogenic sediments in China. Sed. Geol. 261–262, 120–131.

Yang, S., Wang, Q., Lai, X., Qiao, L., Wang, R., Huang, Y., Wang, Y., 2021. Genesis of end-Guadalupian bauxite and pyrite deposits in the Youjiang Basin (South China): insights into the causative link between magmatic events and mass extinction. J. Asian Earth Sci. 215, 104801.

Yu, W., Algeo, T.J., Du, Y., Zhang, Q., Liang, Y., 2016. Mixed volcanogenic-lithogenic sources for Permian bauxite deposits in southwestern Youjiang Basin, South China, and their metallogenic significance. Sed. Geol. 341, 276–288.

Yu, W., Algeo, T.J., Yan, J., Yang, J., Du, Y., Huang, X., Weng, S., 2019. Climatic and hydrologic controls on upper Paleozoic bauxite deposits in South China. Earth Sci. Rev. 189, 159–176.

Zhao, H.N., Xing, L.C., He, H.T., Du, S.J., Ling, K.Y., Wen, H.J., 2022. The mode of occurrence of niobium in bauxite of the Upper Permian Heshan Formation in the Pingguo area, Guangxi Autonomous Region, China. Acta Mineral. Sin. 42 (04), 453–460 in Chinese with English abstract.

Zhong, Y.T., He, B., Xu, Y.G., 2013. Mineralogy and geochemistry of claystones from the Guadalupian-Lopingian boundary at Penglaitan, South China: insights into the pre-Lopingian geological events. J. Asian Earth Sci. 62, 438–462.

Zhong, Y.T., He, B., Mundil, R., Xu, Y.G., 2014. CA-TIMS zircon U-Pb dating of felsic ignimbrite from the Binchuan section: Implications for the termination age of Emeishan large igneous province. Lithos 204, 200–209.